Cell, Vol. 92, 441–450, February 20, 1998, Copyright ©1998 by Cell Press

Crystal Structure of the Tyrosine Phosphatase SHP-2

Peter Hof,*§ Scott Pluskey,*§
Sirano Dhe-Paganon,* Michael J. Eck,†‡
and Steven E. Shoelson*‡
*Joslin Diabetes Center and the Department of Medicine
Harvard Medical School
Boston, Massachusetts 02215
†Dana Farber Cancer Institute and the Department of Biological Chemistry and Molecular Pharmacology
Harvard Medical School
Boston, Massachusetts 02115

Summary

The structure of the SHP-2 tyrosine phosphatase, determined at 2.0 Å resolution, shows how its catalytic activity is regulated by its two SH2 domains. In the absence of a tyrosine-phosphorylated binding partner, the N-terminal SH2 domain binds the phosphatase domain and directly blocks its active site. This interaction alters the structure of the N-SH2 domain, disrupting its phosphopeptide-binding cleft. Conversely, interaction of the N-SH2 domain with phosphopeptide disrupts its phosphatase recognition surface. Thus, the N-SH2 domain is a conformational switch; it either binds and inhibits the phosphatase, or it binds phosphoproteins and activates the enzyme. Recognition of bisphosphorylated ligands by the tandem SH2 domains is an integral element of this switch; the C-terminal SH2 domain contributes binding energy and specificity, but it does not have a direct role in activation.

Introduction

Many cytoplasmic signaling enzymes are both targeted and regulated by interactions of their SH2 domains with phosphotyrosine docking sites created by receptor activation (for reviews, Cohen et al., 1995; Pawson, 1995; Kuriyan and Cowburn, 1997). The SH2 domain phosphatases (SHP-1, SHP-2, and *csw*, a *Drosophila melanogaster* homolog) provide prime examples of this effect. These proteins share a common architecture comprising two SH2 domains followed by a tyrosine phosphatase (PTP) domain, and a C-terminal extension. SHPs are essentially inactive under basal conditions, but catalytic activity (k_{cat}) increases dramatically in parallel with SH2 domain occupancy (Lechleider et al., 1993; Sugimoto et al., 1993; Townley et al., 1993; Dechert et al., 1994; Pei et al., 1994, 1996; Pluskey et al., 1995; Eck et al., 1996). Single phosphopeptides that bind one SH2 domain stimulate PTP activity about 10-fold. Relevant bisphosphoryl sequences that bind both SH2 domains stimulate catalysis up to 100-fold and at much lower peptide concentrations. Several other signaling enzymes are regulated by their SH2 domains, including PI 3-kinase, PLC-γ1, and Syk (Backer et al., 1992; Carpenter et al., 1993; Rowley et al., 1995; Shiue et al., 1995; Rhee and Bae, 1997). Mechanisms for peptide recognition by SH2 domains are well established (reviewed in Kuriyan and Cowburn, 1997), but mechanisms for catalytic regulation by these domains are not known.

Biological functions of the SHP proteins have been extensively reviewed (Tonks, 1996; Neel and Tonks, 1997). SHP-2 is expressed in every tissue and transmits signals in cells that are activated by various ligands, including growth factors, cytokines, hormones, and MHC-antigen complexes. SHP-1 expression is limited primarily to hematopoietic and epithelial cells. SHP-2 (or *Csw*) is critical for normal development in *Xenopus laevis* (Tang et al., 1995; O'Reilly and Neel, 1998) and *Drosophila* (Perkins et al., 1992; Allard et al., 1996); mice that are homozygous for mutant or null SHP-2 alleles die in utero (Arrandale et al., 1996; Saxton et al., 1997). In addition to binding activated receptors, SHP-2 binds receptor substrates like IRS-1 (Kuhne et al., 1993) and several recently identified adhesion molecules, including membrane-spanning SHPS/SIRP and PECAM proteins (Fujioka et al., 1996; Jackson et al., 1997; Kharitonenkov et al., 1997). To understand how the phosphatase activity of SHP-2 is regulated by interaction of its SH2 domains with these phosphoproteins, we have determined the structure of SHP-2.

Results and Discussion

The crystallized protein (residues 1–527) comprises the two SH2 domains and the entire catalytic PTP domain of human SHP-2 but lacks the 66-residue C-terminal tail. The truncated protein is activated by phosphopeptides like the full-length enzyme (data not shown). The structure has been refined to a crystallographic R value of 20%, using data to 2.0 Å resolution. Structure determination and refinement statistics are presented in Table 1. A portion of the electron density map and refined atomic model are shown in Figure 1A.

Domain Organization and Structure

The crystal structure reveals a "closed" domain arrangement in which the two SH2 domains contour around the phosphatase domain (Figures 2A and 2B). The N-terminal SH2 domain binds intramolecularly to the PTP domain; it interacts extensively with the catalytic domain and directly blocks the phosphatase active site. The C-terminal SH2 domain is tethered to the adjacent domains by peptide backbone but does not share a significant interface with either the N-terminal SH2 domain or the PTP domain. The phosphopeptide binding sites of both SH2 domains face away from the phosphatase domain and are fully exposed on the surface of the molecule. A distinct, nonoverlapping surface of the N-terminal domain creates the specific interface with the PTP domain. Although the domains are compactly organized, they appear to interact only loosely. The majority of interdomain contacts are polar, and numerous

‡To whom correspondence should be addressed.
§These authors contributed equally.

Table 1. Data Collection, Structure Determination, and Refinement Statistics

Data Collection	
Space group	$P2_1$
Unit cell	a = 45.63 Å, b = 213.02 Å, c = 55.41 Å $\alpha = \gamma = 90°$, $\beta = 96.3°$
Reflections (observed/unique)	276,084/71,634
R_{merge}	6.17% (29.6% in outer 2.1-2.0 Å shell)
Completeness	93.9% (82.5% in outer 2.1–2.0 Å shell)
Refinement	
Resolution	8.0–2.0 Å
R_{cryst}/R_{free} ($I > 1\sigma$)	22.8/29.0
Number of reflections used	62,840
R_{cryst}/R_{free} ($I > 2\sigma$)	19.9/27.0
Number of reflections used	47,820
RMS deviation (bonds/angles)	0.009 Å/1.5°
B value (average/bonded SD)	28.0 Å^2/1.76 Å^2

water molecules bind in the interfaces between all domains. The polar nature of the intersubunit contacts is consistent with the notion that these interfaces will become fully solvent exposed in the active form of the enzyme.

The PTP domain of SHP-2 has a mixed α/β architecture (Figures 2A and 3) that closely resembles the catalytic domains of PTP1B, Yersinia PTP, PTPα, and PTPμ (Barford et al., 1994; Stuckey et al., 1994; Bilwes et al., 1996; Hoffmann et al., 1997); 203 core α carbons of the SHP-2 and PTPα catalytic domains superimpose with an rmsd of 0.66 Å. The PTP domain of SHP-2 contains nine α helices and 14 β strands. Ten of the β strands form a mixed parallel/antiparallel β sheet that wraps around helix αE. Helices A, B, F, G, H, I, and J pack together on the opposite side of the large β sheet. Catalytic mechanisms for PTPs are well established. Residues of the PTP signature motif, [I/V]HCxAGxxR[S/T]G (single letter code; x = any amino acid), are found in βM and αG and the MG loop between them. Strand βM is at the center of the ten-stranded β sheet. The essential nucleophilic cysteine and all functional groups required for phosphate binding are in the signature motif. These and other residues form a catalytic cleft at the base of the phosphotyrosine binding pocket that extends to a depth of up to 9 Å from the molecular surface.

The N- and C-terminal SH2 domains have the conserved SH2 fold, which consists of a central four-stranded β sheet that is flanked at either surface by an α helix. Phosphopeptides bind to SH2 domains in an extended conformation, with the phosphotyrosine in a pocket on one side of the central sheet and C-terminal residues within a pocket or groove created by the EF and BG loops on the opposite side of the central sheet. The phosphopeptide recognition sites of both SH2 domains are empty, because no ligands were included in the crystallization.

The relative orientation of the two SH2 domains observed here is different from that in our previous structure of a "tandem-SH2" domain fragment of SHP-2 (Eck et al., 1996). In the tandem-SH2 structure, a disulfide bond and a small hydrophobic interface between the domains stabilizes an antiparallel orientation of the two phosphopeptide binding sites, which are about 40 Å apart. In the current structure, there is only a minimal polar interface between the domains, and the cysteines are reduced. As in the tandem-SH2 structure, the phosphopeptide binding sites in SHP-2 are widely separated (over 50 Å between the phosphotyrosine pockets), but they are roughly perpendicular to one another (Figure 2B). The divergence in SH2 domain orientations demonstrates that in the activated form, the domains are likely to be flexible, rather than rigidly fixed with respect to one another, as we previously suggested (Eck et al., 1996).

The Mechanism of Inhibition

The structure reveals a clear mechanism for catalytic inhibition; the N-terminal SH2 domain directly blocks the enzyme active site (Figures 1, 2 and 4). The N-SH2 and the PTP share a broad interaction surface of approximately 1208 Å^2 at each surface (Figure 5). The D′E loop and flanking D′ and E strands of the N-SH2 domain are central to this interaction, and they extend deep into the catalytic cleft. Key conserved features of the PTP catalytic cleft include Cys459, the catalytic nucleophile; Arg465 and the "phosphate binding cradle" formed by several mainchain amide groups in the signature motif, which together coordinate the phosphate oxygens of the bound substrate; and the WPD loop, which closes around the bound phosphotyrosyl substrate and contributes Asp425, the general acid in catalysis (Barford et al., 1994; Stuckey et al., 1994; Jia et al., 1995). In our autoinhibited structure, all of these residues are occupied by interaction with the N-SH2 domain (Figures 1B, 4, and 5). The active site moieties that are expected to hydrogen bond to phosphate oxygens interact instead with the N-SH2 domain or with one of three tightly bound water molecules that are coordinated between the SH2 and the PTP active site (Figures 1A and 1B). Side chains of SH2 domain Asp61 and PTP domain Cys459 are hydrogen bonded through one of these water molecules. An intricate intra- and interdomain hydrogen bonding network, which involves Gly60, Asn58, Gln506, Ala72, and Gly503, stabilizes the D′E loop in the enzyme active site (Figure 1B).

Substrate binding causes a conformational reorganization of the WPD loop in PTP active sites (Stuckey et al., 1994; Jia et al., 1995). In PTP1B, a backbone motion of greater than 5 Å brings Asp181 (the general acid) and Phe182 into the catalytic active site to participate in catalysis and substrate binding (Figure 4). In SHP-2,

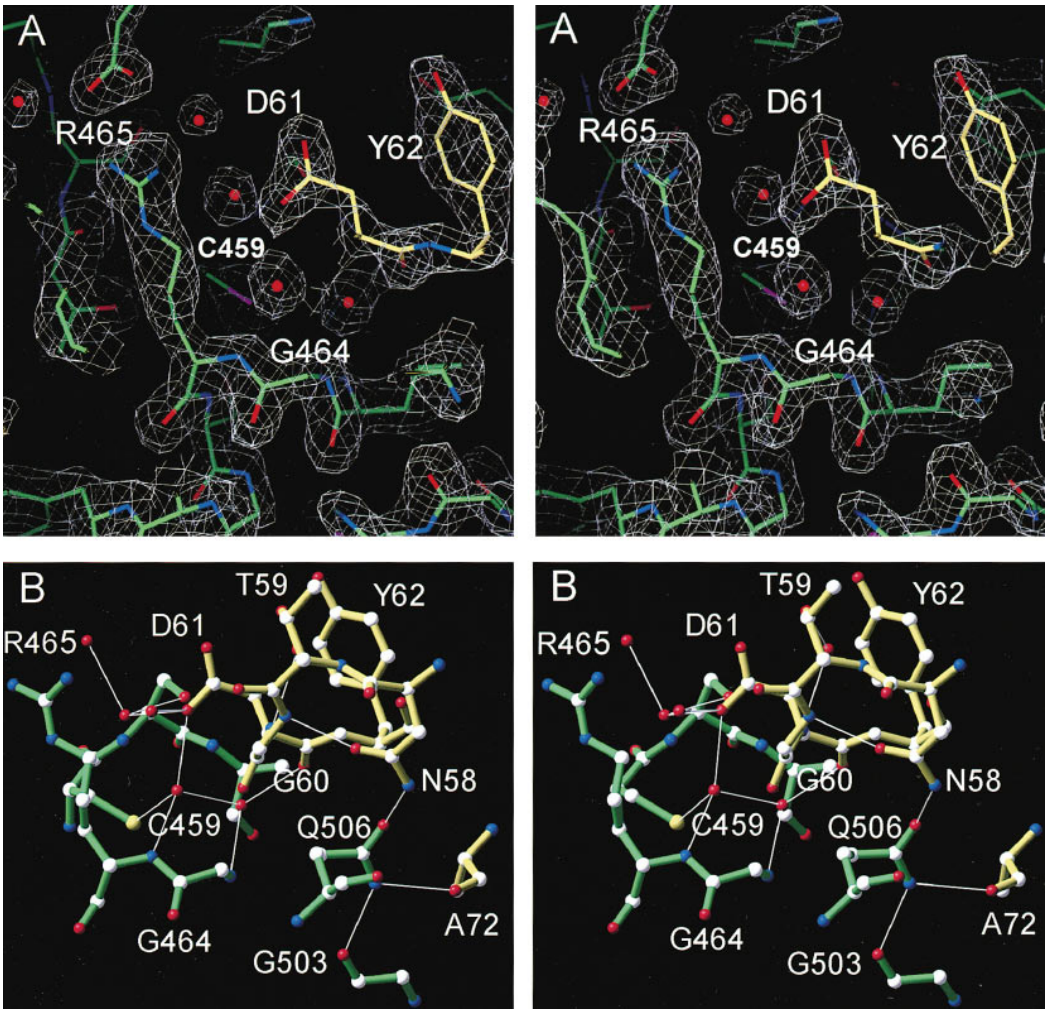

Figure 1. Stereo Figures in the Region of the SHP-2 Active Site

Residues of the phosphatase and N-SH2 domain are oriented similarly and colored green and yellow, respectively, in (A) and (B). Red, oxygen atoms; blue, nitrogens; red spheres, ordered water molecules.

(A) The $2F_o$-F_c electron density map and refined atomic model at the interface of the N-SH2 domain and PTP active site. The map is contoured at 1.3 σ and was calculated using data between 8.0 and 2.0 Å resolution.

(B) Numerous hydrogen bonds (thin white lines) stabilize the interface between the N-SH2 domain and PTP active site.

even though the D′E loop of the SH2 domain occupies the substrate binding site and mimics some features of phosphotyrosine binding, it does not induce closure of the WPD loop. In fact, the bulky D′E turn (Asn58, Thr59, and Gly60) prevents closure of the WPD loop and maintains the active site in the open, inactive conformation seen in PTPs without bound substrate (Figure 4). The receptor-like phosphatase PTPα appears to be regulated by a related steric block of its active site (Bilwes et al., 1996). The proximal PTP domain of PTPα crystallizes as dimer, with the turn connecting helices αA and αB of one molecule inserted into the catalytic cleft of the other. As in SHP-2, this occludes the catalytic site and prevents rearrangement of the WPD loop.

Outside the catalytic cleft proper, a number of polar interactions stabilize the inhibitory interaction. In the N-SH2 domain, residues of helix αB and strands βA, βD′, βE, and βF contribute to the extensive interaction (Figure 5). The complementary surface on the PTP domain is formed by residues of αB and αC and the DB and αHI loops. Specific interactions include a salt bridge between the side chains of Arg4 and Glu258 and hydrogen bonds from Asn281 to Glu69, from Ser502 to Glu76, and from Gln506 to Ala72. If the structure of substrate-bound PTP1B (Jia et al., 1995) predicts the orientation of substrate peptide binding by SHP-2, then the SH2 domain in our structure binds where substrate residues C-terminal to phosphotyrosine would otherwise bind.

Sequence alignments of over 70 known SH2 domains suggest that the interaction between the PTP and SH2 domains in our structure is specific. The “NxGDY/F” sequence motif of βD′-D′E-βE (which inserts deep into the PTP catalytic cleft) is unique to the N-SH2 domains of SHP-1, SHP-2, and *csw* (Figure 3). These enzymes must be regulated by a similar mechanism. Asn58 in this motif is key to the SH2-PTP hydrogen bonding network

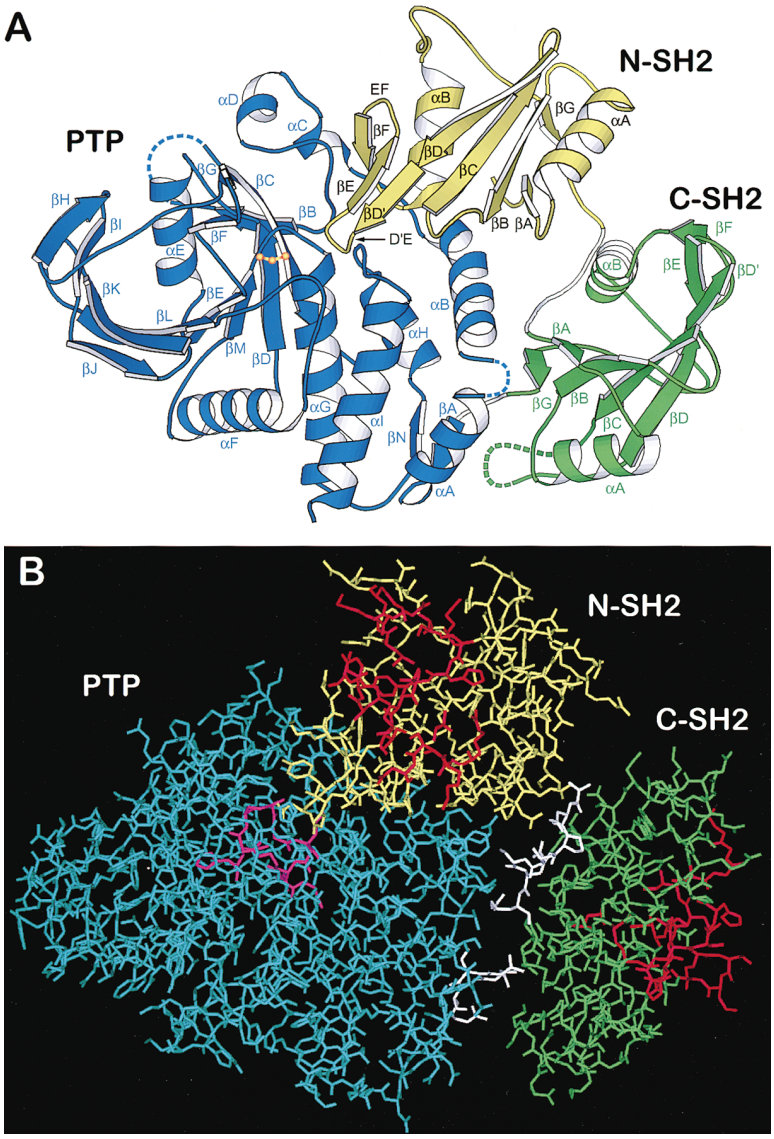

Figure 2. The Structure of SHP-2 in Its Autoinhibited, Closed Configuration

Structures in (A) and (B) are in similar orientations. The N- and C-terminal SH2 domains are yellow and green, respectively; the catalytic PTP domain is blue, and interdomain linkers (residues 104–111 and 217–220) are white in both panels.

(A) Richardson diagram showing secondary structure and organization of the domains. Orange, the side chain of Cys459 (the catalytic nucleophile); dashed lines, disordered loops.

(B) All nonhydrogen atoms of SHP-2 are displayed. Although SH2 domain–bound peptides are not present in our structure, residues of both domains known to contact phosphopeptides (Lee et al., 1994; Eck et al., 1996) are colored red. Note that peptide binding sites of both SH2 domains are exposed on the molecule surface. A distinct surface of the N-SH2 domain occupies the active site of the PTP domain. Magenta, residues of the PTP signature motif, HCSAGIGRS; these residues participate in catalysis and phosphate binding.

(Figure 1B) and is not found at this position in any other SH2 domain. The Gly in this motif may be required because the bond angles it adopts are not allowed for chiral amino acids ($\psi = 134°$, $\phi = -11.7°$). As discussed above, Gly60 and Asp61 set up the hydrogen bond network to Cys459 (Figure 1B). The aromatic residue that completes the motif (Tyr62 in SHP-2) is probably required for binding the hydrophobic portion of the PTP domain phosphotyrosine-binding site (Figure 4).

The N-SH2 Domain Is a Molecular Switch

Given that separate surfaces of the N-SH2 domain interact with phosphopeptide and the PTP domain, how does phosphoprotein binding to the SH2 domains activate catalysis? The structure of SHP-2 shows that its N-SH2 domain functions as an "allosteric" switch. Binding of a phosphopeptide ligand at one site induces a transmitted conformational change that prevents PTP domain binding at a second site, and vice versa. Comparison of the N-SH2 domain in our structure with previously determined structures of the domain (Lee et al., 1994; Eck et al., 1996), both free and in complex with phosphopeptides, reveals these differences in conformation (Figure 6). In particular, the positions of the B helix and the secondary β sheet (strands βD′, βE, and βF) change with respect to the A helix and the central sheet, which remain fixed. The secondary β sheet and B helix interact directly with the PTP domain. The change in position and conformation of these elements upon phosphopeptide binding disrupts the inhibitory interaction with the PTP domain. We refer to the isolated, phosphopeptide-bound conformation, which promotes activation of the phosphatase, as the "A" state and the PTP associated, inhibitory conformation as the "I" state. Their superposition (Figure 6A) shows that in the I state, the B-helix is displaced along its axis toward its C-terminal end by approximately 2 Å. The secondary β sheet is displaced as well, and this is accompanied by changes in its structure at both the PTP and phosphopeptide binding surfaces. The D′E turn is displaced by its insertion into the PTP active site, and the EF loop folds in toward the BG loop, blocking the phosphopeptide binding groove of

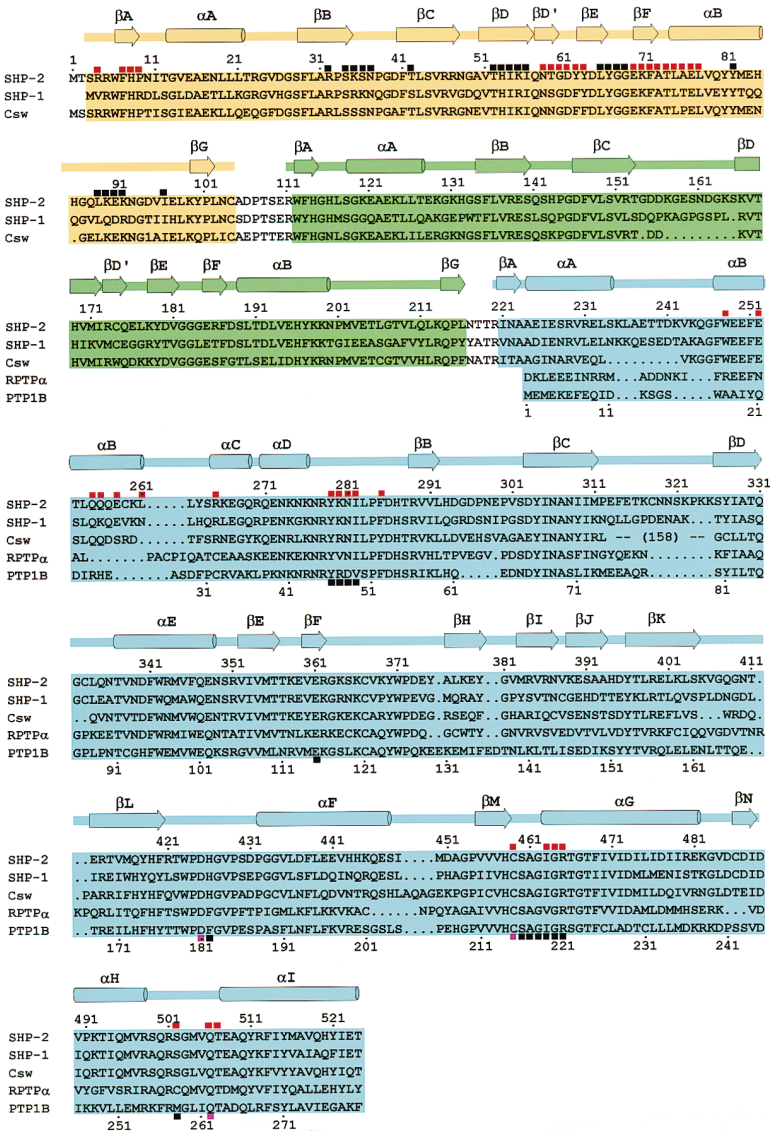

Figure 3. Structure-Based Sequence Alignment of SHP-2 and Other Tyrosine Phosphatases

Sequences are of human SHP-2 and SHP-1, *csw*, and the PTP domains of human PTPα and PTP1B. Elements of SHP-2 secondary structure are shown above the alignment. Regions corresponding to the N-SH2, C-SH2, and phosphatase domains are colored as in Figure 2. Red squares, residues of the SHP-2 N-SH2 and PTP domains that bind each other; black squares, residues of the SHP-2 N-SH2 domain or PTP1B catalytic domain that bind phosphopeptide; lavender squares, catalytic residues of PTP1B. Residue numbers for SHP-2 and PTP1B are above and below the alignment, respectively.

the SH2 domain (Figure 6B). The mainchain of the EF loop (Tyr66-Gly67-Gly68) shifts by as much as 5.1 Å, relative to its position in the A state. The isolated, unliganded N-SH2 domain is essentially in the A state (Lee et al., 1994). Prior structures of the N-SH2 domain alone did not reveal this switch, because the second conformation, the inhibitory I state, is induced by interaction with the PTP domain.

We previously noted that the position of the B-helix in the liganded N-SH2 domain is divergent from that of other SH2 domains, and we suggested that this might result from substitution of an alanine for the usual valine at position βB4 (valine in the conserved "FLVRES" signature motif) (Eck et al., 1996). Alanine at this position is unique to the N-terminal SH2 domains of the SH2 phosphatases. Over 70 other SH2 domains, including the C-terminal domains of these enzymes, contain Val, Ile, or Leu at this position. The bulky βB4 sidechain contributes to the hydrophobic core of other domains, and it appears to fix the position of the B helix with respect to the central β sheet by interacting with other core residues. Because alanine at the βB4 position is not compensated by observable "second-site mutations," this leaves a cavity in the N-SH2 domain. Similar cavities render alternative proteins 2.5–5 kcal/mol less stable (Eriksson et al., 1992; Jackson et al., 1993a, 1993b; Baldwin et al., 1996). In the N-SH2 domain this may "loosen up" core packing to allow the apparent sliding of the B helix. As a simple mechanical analogy, the substitution could "unlock" the B helix by removing the larger sidechain, which would otherwise interdigitate with the sidechains of the B helix, to fix its position relative to the central sheet. Therefore, the alanine at position βB4 may permit the formation of distinct I and A states and facilitate interconversion by reducing the magnitude of the energy barrier between them.

A Model for SHP-2 Regulation

The conformational switch described above, together with available biochemical data, suggests a model for SHP-2 regulation. The N-SH2 domain has two ligands,

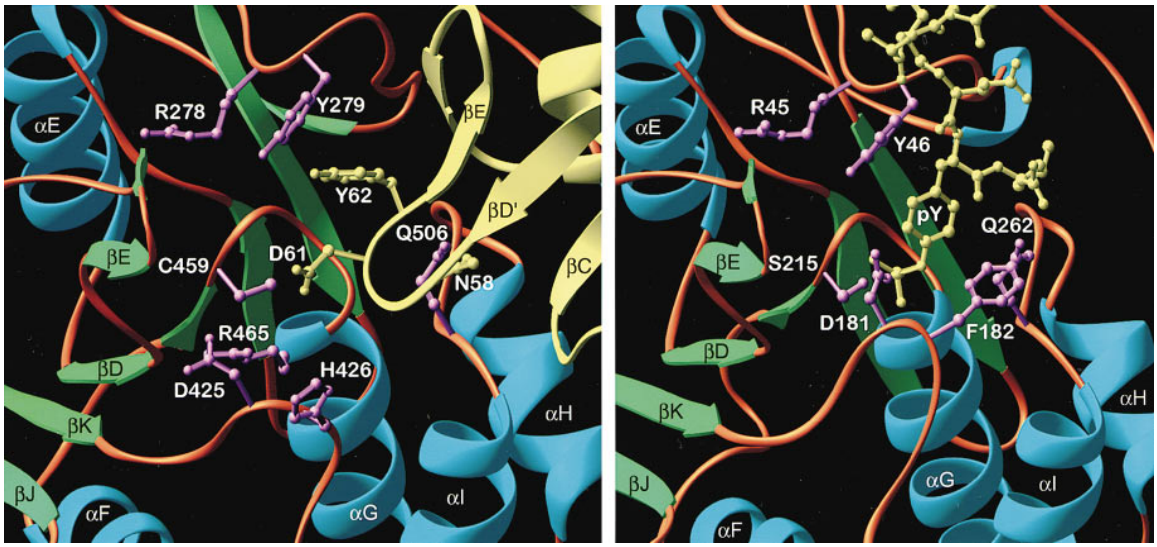

Figure 4. PTP Inhibition Compared to Substrate Recognition

The PTP domains of SHP-2 (left) and PTP1B (right) are shown in identical orientations. Turquoise, α helices; green, β strands; brown, intervening random coils; lavender ball-and-stick models, side chains of key PTP residues; yellow, the SH2 domain in the SHP-2 structure (left) and the phosphopeptide substrate in the PTP1B structure (right). Note that the SH2 domain occupies the entire phosphotyrosine-binding site.

which bind at nonoverlapping sites: an intermolecular interaction with phosphopeptide, and an intramolecular interaction with the PTP domain. These sites apparently interact with negative cooperativity. Under basal conditions, in the absence of SH2 domain–binding partners, the concentration of closed SHP-2 greatly exceeds that of the open form, as evidenced by very low catalytic activity of the unliganded protein. In the phosphopeptide-bound A state, the affinity of the N-SH2 domain for the PTP is diminished. This effect has been demonstrated directly using isolated SHP-2 SH2 and PTP domains (Dechert et al., 1994). Further, our structural analysis shows that in the A state, the N-SH2 domain loses surface complementarity for its binding site on the PTP (Figure 6A). Thus phosphopeptide binding promotes intramolecular "dissociation" of the N-SH2 from the PTP, shifting the equilibrium to an open conformation in which the steric block of the catalytic site is relieved and SHP-2 is catalytically active.

Thermodynamic considerations require that the converse must also be true: interaction of the N-SH2 with the PTP must diminish its affinity for phosphopeptide. We see the structural manifestations of the diminished affinity of the I state for phosphopeptide—most obviously the closed EF loop, which partially blocks the peptide binding groove (Figure 6B). This observation illuminates the role of the C-SH2 domain and two-site, tandem SH2 domain–binding in enzymatic activation

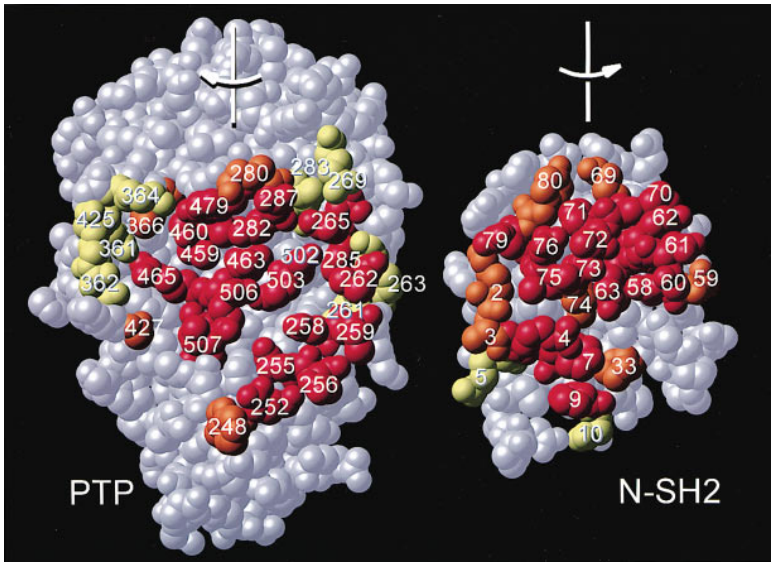

Figure 5. The N-SH2 Domain-PTP Domain Interface Viewed as an "Open Book"

The PTP (left) and N-SH2 (right) are both rotated 90° but in opposite directions to expose the buried surface between them. Contact residues are numbered and color-coded to reflect the percentage of surface buried (red, 50%–100%; orange, 25%–50%; yellow, 0%–25%).

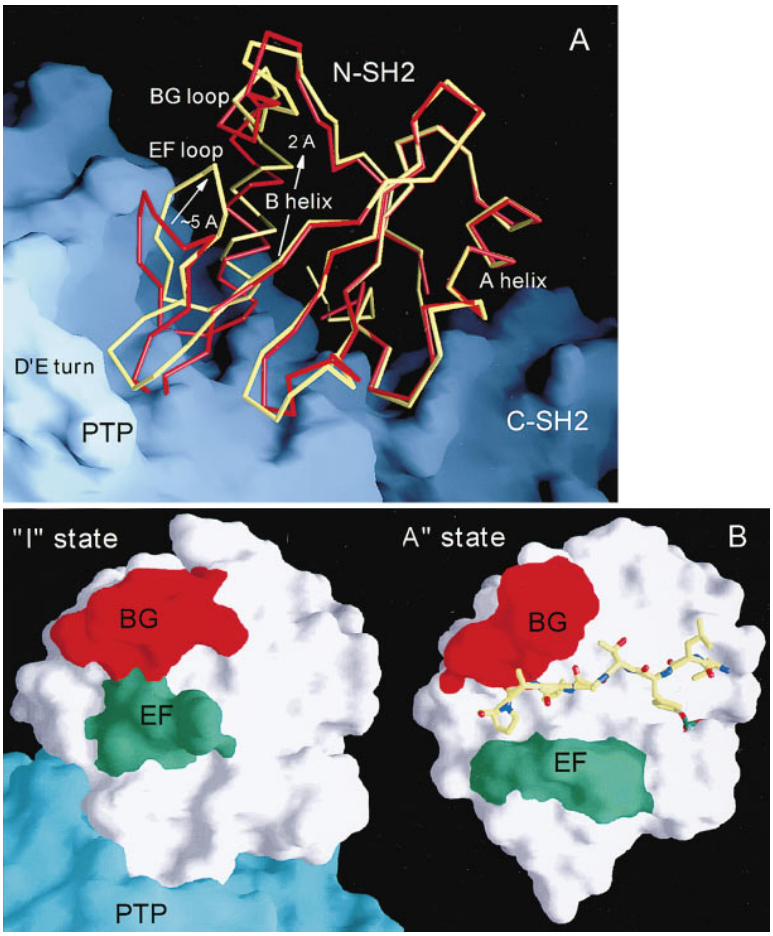

Figure 6. A Conformational Change in the N-SH2 Domain Regulates SHP-2

(A) An α-carbon trace of the phosphopeptide-bound A conformation of the N-SH2 domain (red) (Eck et al., 1996) is superimposed on the I state domain in the present structure (yellow). The domains were superimposed using the invariant portions of the structure (residues 6–55) as determined by analysis of difference distance matrix plots with the program DDMP (Richards and Kundrot, 1988). The molecular surface of the PTP and C-SH2 domains is shown in blue. Note that in the peptide-bound A state, the N-SH2 backbone (red) would collide with the surface of the PTP domain.

(B) Molecular surfaces of the N-SH2 domain from the SHP-2 structure (I state) and the isolated SH2 domain bound to a phosphopeptide (A state) (Lee et al., 1994); the domains are oriented similarly according to elements of secondary structure. Residues of the EF (66–68) and BG (89–92) loops are green and red, respectively. A stick figure with carbon colored white, the PDGFR 1009 peptide; blue, nitrogen; red, oxygen; yellow, phosphorus. Closure of the EF and BG loops in the I state precludes high-affinity phosphopeptide binding. The change in shape of the N-SH2 domain that accompanies phosphopeptide binding destroys surface complementarity for the PTP active site. Phosphopeptide binding thus promotes dissociation of the N-SH2 and PTP domains to generate the active A state of SHP-2.

and biological function. By binding one site in a bisphosphoryl ligand, the C-SH2 domain provides binding energy and increases the local concentration of ligand so that the compromised N-SH2 domain can bind a second site. Upon binding to the second site, the N-SH2 domain adopts the A state; this shifts the equilibrium to the open, active form of the PTP. Engagement of the C-SH2 domain alone is unlikely to contribute to activation, because it makes only minimal contact with the other domains. Although high concentrations of a monophosphotyrosyl ligand can overcome the diminished affinity of the N-SH2 domain and activate SHP-2 in vitro, in the context of cellular signaling, the one-to-one stoichiometry afforded by receptor activation is probably not sufficient to recruit and activate SHP-2 via the N-SH2 alone.

The great distance between SH2 domain–binding sites—over 50 Å between phosphotyrosine binding sites in this structure—undoubtedly contributes to specificity. Phosphotyrosines within SHP-1/SIRP proteins are separated by 23–25 residues, and relevant sites in IRS-1 are even further apart (49 residues). SHP-2 binds corresponding bisphosphoryl peptides from these biological partners with high affinity (K_D ~1 nM). In contrast, tandem SH2 domains from alternative signaling proteins (PI 3-kinase p85, ZAP-70, Syk, and PLCγ) bind with 1,000 to less than 10,000-fold lower affinity (Ottinger et al., 1998). These other tandem SH2 domain proteins bind distinct bisphosphotyrosyl sequences derived from their own biological partners, and tyrosines in these sequences are separated by much shorter distances (9–11 residues between tyrosines in T cell receptor and FcεRI TAMs and related sites in the PDGF receptor) (Ottinger et al., 1998). SHP-2 does not bind these alternative ligands, because phosphotyrosines within them are too close together. However, SHP-2 is activated by homodimeric receptors such as the PDGF receptor that have single recognition sites in each receptor monomer. Presumably, the SH2 domains in SHP-2 bridge the dimer by binding equivalent sites on each monomer.

What role does the C terminus of SHP-2 play in enzymatic activation and biological function? SHP-2 may be activated by limited proteolysis (Sugimoto et al., 1994). Based on the mapping of a tryptic cleavage site to the C terminus of SHP-2, it was concluded that the C terminus acts along with the SH2 domains to regulate catalysis. However, engineered enzymes corresponding to truncations around the tryptic site (e.g., 1–537; Sugimoto et al., 1994) and shorter forms including the one used here (1–527) all show activation profiles like the wild-type protein. The C-terminal extension is phosphorylated in activated cells (Feng et al., 1993; Vogel et al., 1993) and may be a docking site for SH2 domain proteins (Welham et al., 1994). However, the phosphorylation sites can be eliminated without an apparent loss of function in

transfected cells (Bennett et al., 1996) and injected frog embryos (Tang et al., 1995; O'Reilly and Neel, 1998). Genetic studies in *Drosophila* suggest that the entire C-terminal tail of *csw* is dispensable (Michael Simon, personal communication). Our structure lacks the C-terminal extension and therefore provides no direct information about its potential functions.

Conclusions

Although many signaling enzymes, including tyrosine kinases, lipid kinases, and phospholipases, are constructed with structurally homologous modular domains, it is clear that distinct mechanisms must have evolved to control their activities. Comparison of the regulatory mechanisms employed in SHP-2 and in the Src-family tyrosine kinases, the other class of SH2-regulated enzyme for which structural detail is available (Sicheri et al., 1997; Williams et al., 1997; Xu et al., 1997), shows how divergent structural mechanisms produce related regulatory effects. In the Src kinases, the SH2 domain binds intramolecularly to the phosphorylated tail of the protein, and the SH3 domain binds to a linker segment. These interactions effectively clamp the two lobes of the tyrosine kinase together in a manner that disrupts the active site and simultaneously blocks the ligand binding surfaces of the SH3 and SH2 domains. The single-domain architecture of the phosphatase domain requires a more direct form of inhibition: a steric block of the catalytic cleft by the SH2 domain. Despite dramatically different mechanisms and distinct architectures, the SH2 domain phosphatases and Src-family kinases are both constructed and "tuned" such that high-affinity, intermolecular binding is required to break the inhibitory intramolecular effects of the targeting domains. In both cases, intracellular targeting and enzyme activation are intimately coupled. This is likely a common theme in signaling proteins.

Experimental Procedures

Crystallization of SHP-2

Recombinant human SHP-2 (residues 1–527) was expressed in *Escherichia coli* and isolated by sequential column chromatography using phosphotyrosine-Sepharose (Eck et al., 1996), Mono-Q (Pharmacia), and Superdex 200 (Pharmacia). Crystals were grown at room temperature by vapor diffusion in sitting drops containing equal volumes of protein solution (15 mg/ml in 100 mM NaCl, 100 mM Tris [pH 8.5], and 20 mM dithiothreitol) and reservoir solution (13% PEG 4000, 100 mM Tris [pH 8.5], and 20 mM dithiothreitol). Addition of trimethyl lead acetate (5 mM) and cetyltrimethylammonium bromide (CTAB, 1.2 mM) to the drops enhanced the growth of single, well-ordered crystals. Macroseeding was required to obtain crystals of sufficient size (0.2 × 0.3 × 0.6 mm). The crystals belong to the monoclinic space group $P2_1$ and contain 2 molecules per asymmetric unit. Crystals were transferred stepwise into reservoir buffer containing glycerol (final concentration 20%) for cryogenic data collections.

Data Collection and Structure Determination

Diffraction data from a single crystal were recorded with MarResearch Image Plate detector mounted on a Rigaku rotating anode with mirror optics; the data were integrated and scaled with the programs XDS and XSCALE (Kabsch, 1988). The structure of SHP-2 was determined by molecular replacement using the programs AMoRe (Navaza, 1992) and X-PLOR (Brunger, 1992). Unambiguous solutions to rotational and translational searches were obtained for the PTP domain portion of the structure using the coordinates of PTP1B (Barford et al., 1994) (with side chains of nonconserved residues converted to L-Ala) as a search model. With consideration of crystal packing constraints and noncrystallographic symmetry operators, correct molecular replacement solutions for the N-terminal SH2 domains (Lee et al., 1994) were identified, but we were unable to position the C-terminal SH2 domains. Electron density maps phased with the partial replacement model were improved with iterative, real-space noncrystallographic symmetry averaging, solvent flattening, and histogram matching using the program DM (Cowtan, 1994) and associated programs in the CCP4 package (Collaborative Computational Project 4, 1994). Averaging masks were positioned in the region of the C-SH2 domain and manually edited. The improved, averaged maps allowed construction of the C-SH2 domain and segments of the polypeptide chain linking the SH2 and PTP domains. The model was refined to a crystallographic *R* value of 19.9% (R_{free} = 27.0%) with manual refitting, conjugate gradient minimization, and simulated annealing with programs MAIN (Turk, 1996), O (Jones et al., 1989), and X-PLOR (Brunger, 1992). Tight noncrystallographic symmetry restraints were maintained throughout the refinement. There are no obvious differences between molecules in the asymmetric unit; rms differences between selected atoms of each of the two N-SH2, C-SH2, and PTP domains in the asymmetric unit are 0.0352 Å, 0.0280 Å, and 0.0383 Å, respectively. Water molecules were added with the aid of the program ARP (Lamzin and Wilson, 1993). The crystallized protein differs from the published sequence at three sites: Thr2Lys, Phe41Leu, and Phe513Ser. The cavity left by mutation of Phe513 binds a detergent molecule, but the mutations do not otherwise alter the structure (the corresponding wild-type SHP-2 fragment crystallizes isomorphously, but suitable crystals for structure determination were not obtained). The final model contains 7928 protein atoms (2 SHP-2 molecules), 777 solvent molecules, and 2 detergent molecules (CTAB). All residues in both proteins of the asymmetric unit are identified except residues 156–160, 236–245, 295–301, and 313–323. These three disordered loops in the PTP domain and one in the C-terminal SH2 domain are not involved in catalytic or known binding functions of the protein.

Figures 1B, 4, and 5 were prepared using the program RIBBONS (Carson, 1991); Figure 1A was made with O (Jones, 1989); Figure 2B was made with MAIN (Turk, 1996); Figure 2A was made with MOLSCRIPT (Kraulis, 1991); and Figures 6A and 6B were made with GRASP (Nicholls et al., 1991). Coordinates have been deposited at the PDB in Brookhaven under code 2SHP and can be obtained by e-mail from eck@red.dfci.harvard.edu or shoelson@joslab.harvard.edu.

Acknowledgments

The authors thank S. Harrison, B. Neel, and C. Walsh for helpful discussions and advice. Financial support for these studies was provided by the National Institutes of Health and the Burroughs Wellcome Fund.

Received December 16, 1997; revised January 27, 1998.

References

Allard, J.D., Chang, H.C., Herbst, R., McNeill, H., and Simon, M.A. (1996). The SH2-containing tyrosine phosphatase corkscrew is required during signaling by sevenless, Ras1 and Raf. Development *122*, 1137–1146.

Arrandale, J.M., Gore-Willse, A., Rocks, S., Ren, J.M., Zhu, J., Davis, A., Livingston, J.N., and Rabin, D.U. (1996). Insulin signaling in mice expressing reduced levels of Syp. J. Biol. Chem. *271*, 21353–21358.

Backer, J.M., Myers, M.G., Shoelson, S.E., Chin, D.J., Sun, X.J., Miralpeix, M., Hu, P., Margolis, B., Skolnik, E.Y., Schlessinger, J., and White, M.F. (1992). Phosphatidylinositol 3′-kinase is activated by association with IRS-1 during insulin stimulation. EMBO J. *11*, 3469–3479.

Baldwin, E., Xu, J., Hajiseyedjavadi, O., Baase, W.A., and Matthews, B.W. (1996). Thermodynamic and structural compensation in "size-switch" core repacking variants of bacteriophage T4 lysozyme. J. Mol. Biol. *259*, 542–559.

Barford, D., Flint, A.J., and Tonks, N.K. (1994). Crystal structure of human protein tyrosine phosphatase 1B. Science *263*, 1397–1404.

Bennett, A.M., Hausdorff, S.F., O'Reilly, A.M., Freeman, R.M., and Neel, B.G. (1996). Multiple requirements for SHPTP2 in epidermal growth factor-mediated cell cycle progression. Mol. Cell Biol. *16*, 1189–1202.

Bilwes, A.M., den Hertog, J., Hunter, T., and Noel, J.P. (1996). Structural basis for inhibition of receptor protein-tyrosine phosphatase-α by dimerization. Nature *382*, 555–559.

Brunger, A.T. (1992). X-PLOR Version 3.1: A System for X-ray Crystallography and NMR (New Haven, Connecticut: Yale University).

Carpenter, C.L., Auger, K.R., Chaudhuri, M., Yoakim, M., Schaffhausen, B., Shoelson, S.E., and Cantley, L.C. (1993). Phosphoinositide 3-kinase is activated by phosphopeptides that bind to the SH2 domains of the 85 kDa subunit. J. Biol. Chem. *268*, 9478–9483.

Carson, M. (1991). Ribbons 2.0. J. Appl. Cryst. *24*, 958–961.

Cohen, G.B., Ren, R., and Baltimore, D. (1995). Modular binding domains in signal transduction proteins. Cell *80*, 237–248.

Collaborative Computational Project 4 (1994). The CCP4 suite: programs for protein crystallography. Acta Cryst. *D50*, 760–776.

Cowtan, K. (1994). "DM": an automated procedure for phase improvement by density modification. Joint CCP4 and ESF-EACBM Newsletter on Protein Cryst. *31*, 34–38.

Dechert, U., Adam, M., Harder, K.W., Clark-Lewis, I., and Jirik, F. (1994). Characterization of the protein tyrosine phosphatase SH-PTP2. Study of phosphopeptide substrates and possible regulatory role of the SH2 domains. J. Biol. Chem. *269*, 5602–5611.

Eck, M.J., Pluskey, S., Trub, T., Harrison, S.C., and Shoelson, S.E. (1996). Spatial constraints on the recognition of phosphoproteins by the tandem SH2 domains of the phosphatase SH-PTP2. Nature *379*, 277–280.

Eriksson, A.E., Baase, W.A., Zhang, X.J., Heinz, D.W., Blaber, M., Baldwin, E.P., and Matthews, B.W. (1992). Response of a protein structure to cavity-creating mutations and its relation to the hydrophobic effect. Science *255*, 178–183.

Feng, G.S., Hui, C.-C., and Pawson, T. (1993). SH2 containing phosphotyrosine phosphatase as a target of protein-tyrosine kinases. Science *259*, 1607–1614.

Fujioka, Y., Matozaki, T., Noguchi, T., Iwamatsu, A., Yamao, T., Takahashi, N., Tsuda, M., Takada, T., and Kasuga, M. (1996). A novel membrane glycoprotein, SHPS-1, that binds the SH2-domain-containing protein tyrosine phosphatase SHP-2 in response to mitogens and cell adhesion. Mol. Cell. Biol. *16*, 6887–6899.

Hoffmann, K.M., Tonks, N.K., and Barford, D. (1997). The crystal structure of domain 1 of receptor protein-tyrosine phosphatase μ. J. Biol. Chem. *272*, 27505–27508.

Jackson, S.E., elMasry, N., and Fersht, A.R. (1993a). Structure of the hydrophobic core in the transition state for folding of chymotrypsin inhibitor 2: a critical test of the protein engineering method of analysis. Biochemistry *32*, 11270–11278.

Jackson, S.E., Moracci, M., elMasry, N., Johnson, C.M., and Fersht, A.R. (1993b). Effect of cavity-creating mutations in the hydrophobic core of chymotrypsin inhibitor 2. Biochemistry *32*, 11259–11269.

Jackson, D.E., Kupcho, K.R., and Newman, P.J. (1997). Characterization of phosphotyrosine binding motifs in the cytoplasmic domain of platelet/endothelial cell adhesion molecule-1 (PECAM-1) that are required for the cellular association and activation of the protein-tyrosine phosphatase, SHP-2. J. Biol. Chem. *272*, 24868–24875.

Jia, Z., Barford, D., Flint, A.J., and Tonks, N.K. (1995). Structural basis for phosphotyrosine peptide recognition by protein tyrosine phosphatase 1B. Science *268*, 1754–1758.

Jones, T.A., Bergdoll, M., and Kjeldgaard, M. (1989). Crystallographic Computing and Modeling Methods in Molecular Design. C. Bugg and S. Ealick, eds. (New York: Springer).

Kabsch, W.J. (1988). Evaluation of single crystal diffraction data from a position sensitive detector. J. Appl. Cryst. *21*, 916–924.

Kharitonenkov, A., Chen, Z., Sures, I., Wang, H., Schilling, J., and Ullrich, A. (1997). A family of proteins that inhibit signaling through tyrosine kinase receptors. Nature *386*, 181–186.

Kraulis, P.J. (1991). MOLSCRIPT: a program to produce both detailed and schematic plots of protein structures. Appl. Cryst. *24*, 946–950.

Kuhne, M.R., Pawson, T., Lienhard, G.E., and Feng, G.S. (1993). The insulin receptor substrate 1 associates with the SH2-containing phosphotyrosine phosphatase Syp. J. Biol. Chem. *268*, 11479–11481.

Kuriyan, J., and Cowburn, D. (1997). Modular peptide recognition domains in eukaryotic signaling. Annu. Rev. Biophys. Biomol. Struct. *26*, 259–288.

Lamzin, V.S., and Wilson, K.S. (1993). Acta Cryst. *D49*, 129–147.

Lechleider, R.J., Sugimoto, S., Bennett, A.M., Kashishian, A.S., Cooper, J.A., Shoelson, S.E., Walsh, C.T., and Neel, B.G. (1993). Activation of the SH2-containing phosphotyrosine phosphatase SH-PTP2 by its binding site, phosphotyrosine 1009, on the human platelet-derived growth factor receptor β. J. Biol. Chem. *268*, 21478–21481.

Lee, C.-H., Kominos, D., Jaques, S., Margolis, B., Schlessinger, J., Shoelson, S.E., and Kuriyan, J. (1994). Crystal structures of peptide complexes of the N-terminal SH2 domain of the Syp tyrosine phosphatase. Structure *2*, 423–438.

Navaza, J. (1992). Molecular Replacement: Proceedings of the CCP4 Study Weekend. E.J. Dodson, S. Gover, and W. Wolf, eds. (Daresbury, UK: SERC), pp. 87–90.

Neel, B.G., and Tonks, N.K. (1997). Protein tyrosine phosphatases in signal transduction. Curr. Opin. Cell Biol. *9*, 193–204.

Nicholls, A., Sharp, K.A., and Honig, B. (1991). Protein folding and association: insights from the interfacial and thermodynamic properties of hydrocarbons. Proteins Struct. Funct. Genet. *11*, 281–296.

O'Reilly, A.M., and Neel, B.G. (1998). Structural determinants of SHP-2 function and specificity in xenopus mesoderm induction. Mol. Cell. Biol. *18*, 161–177.

Ottinger, E.A., Botfield, M., and Shoelson, S.E. (1998). Tandem SH2 domains confer high specificity in tyrosine kinase signaling. J. Biol. Chem. *273*, 729–733.

Pawson, T. (1995). Protein modules and signaling networks. Nature *373*, 573–580.

Pei, D., Lorenz, U., Klingmuller, U., Neel, B.G., and Walsh, C.T. (1994). Intramolecular regulation of protein tyrosine phosphatase SH-PTP1: a new function for Src homology 2 domains. Biochemistry *33*, 15483–15493.

Pei, D., Wang, J., and Walsh, C.T. (1996). Differential functions of the two Src homology 2 domains in protein tyrosine phosphatase SH-PTP1. Proc. Natl. Acad. Sci. USA *93*, 1141–1145.

Perkins, L.A., Larsen, I., and Perrimon, N. (1992). *corkscrew* encodes a putative protein tyrosine phosphatase that functions to transduce the terminal signal from the receptor tyrosine kinase torso. Cell *12*, 225–236.

Pluskey, S., Wandless, T.J., Walsh, C.T., and Shoelson, S.E. (1995). Potent stimulation of SH-PTP2 phosphatase activity by IRS-1 binding to both of its SH2 domains. J. Biol. Chem. *270*, 2897–2900.

Rhee, S.G., and Bae, Y.S. (1997). Regulation of phosphoinositide-specific phospholipase C isozymes. J. Biol. Chem. *272*, 15045–15048.

Richards, F.M., and Kundrot, C.E. (1988). Identification of structural motifs from protein coordinate data: secondary structure and first-level supersecondary structure. Proteins *3*, 71–84.

Rowley, R.B., Burkhardt, A.L., Chao, H.G., Matsueda, G.R., and Bolen, J.B. (1995). Syk protein-tyrosine kinase is regulated by tyrosine-phosphorylated Ig α/Ig β immunoreceptor tyrosine activation motif binding and autophosphorylation. J. Biol. Chem *270*, 11590–11594.

Saxton, T.M., Henkemeyer, M., Gasca, S., Shen, R., Rossi, D.J., Shalaby, F., Feng, G.S., and Pawson, T. (1997). Abnormal mesoderm patterning in mouse embryos mutant for the SH2 tyrosine phosphatase SHP-2. EMBO J. *16*, 2352–2364.

Shiue, L., Zoller, M.J., and Brugge, J.S. (1995). Syk is activated by phosphotyrosine-containing peptides representing the tyrosine-based activation motifs of the high affinity receptor for IgE. J. Biol. Chem. *270*, 10498–10502.

Sicheri, F., Moarefi, I., and Kuriyan, J. (1997). Crystal structure of the Src family tyrosine kinase Hck. Nature *385*, 602–609.

Stuckey, J.E., Schubert, H.L., Fauman, E.B., Zhang, Z.-Y., Dixon, J.E., and Saper, M.A. (1994). Crystal structure of the Yersinia protein tyrosine phosphatase at 2.5 Å and the complex with tungstate. Nature *370*, 571–575.

Sugimoto, S., Lechleider, R.J., Shoelson, S.E., Neel, B.G., and Walsh, C.T. (1993). Expression, purification and catalytic properties of the SH2 domain-containing protein tyrosine phosphatase, SH-PTP2. J. Biol. Chem. *268*, 22771–22776.

Sugimoto, S., Wandless, T., Shoelson, S.E., Neel, B.G., and Walsh, C.T. (1994). Activation of the SH2-containing protein tyrosine phosphatase, SH-PTP2, by phosphotyrosine-containing peptides derived from IRS-1. J. Biol. Chem. *269*, 13614–13622.

Tang, T.L., Freeman, R.M., Jr., O'Reilly, A.M., Neel, B.G., and Sokol, S.Y. (1995). The SH2-containing protein-tyrosine phosphatase SH-PTP2 is required upstream of MAP kinase for early xenopus development. Cell *80*, 473–483.

Tonks, N.K. (1996). Protein tyrosine phosphatases and the control of cellular signaling responses. Adv. Pharmacol. *36*, 91–119.

Townley, R., Shen, S.-H., Banville, D., and Ramachandran, C. (1993). Inhibition of the activity of protein tyrosine phosphatase 1C by its SH2 domains. Biochemistry *32*, 13414–13418.

Turk, D. (1996). MAIN 96: an interactive software for density modifications, model structure refinement and analysis. In Proceedings from the 1996 Meeting of the International Union of Crystallography and Macromolecular Modeling Computing School.

Vogel, W., Lammers, R., Huang, J., and Ullrich, A. (1993). Activation of a phosphotyrosine phosphatase by tyrosine phosphorylation. Science *259*, 1611–1614.

Welham, M.J., Dechert, U., Leslie, K.B., Jirik, F., and Schrader, J.W. (1994). Interleukin (IL)-3 and granulocyte/macrophage colony-stimulating factor, but not IL-4, induce tyrosine phosphorylation, activation, and association of SHPTP2 with Grb2 and phosphatidylinositol 3′-kinase. J. Biol. Chem. *269*, 23764–23768.

Williams, J.C., Weijland, A., Gonfloni, S., Thompson, A., Courtneidge, S.A., Superti-Furga, G., and Wierenga, R.K. (1997). The 2.35 A crystal structure of the inactivated form of chicken src: a dynamic molecule with multiple regulatory interactions. J. Mol. Biol. *274(5)*, 757–775.

Xu, W., Harrison, S.C., and Eck, M.J. (1997). Three-dimensional structure of the tyrosine kinase c-Src. Nature *385*, 595–602.